2010 IEEE International Conference on Robotics and Automation
Anchorage Convention District
May 3-8, 2010, Anchorage, Alaska, USA

Position Tracking using Adaptive Control for Bilateral Teleoperators with Time-Delays

Emmanuel Nuño[1,2], Luis Basañez[2], Romeo Ortega[3] and Guillermo Obregón-Pulido[2]

***Abstract*— This paper presents two versions of adaptive controllers for nonlinear bilateral teleoperators, each providing asymptotic convergence of velocity and position errors to zero, independent of constant time-delays. Moreover, the proposed schemes do not rely on the use of the scattering transformation. The paper also proves that the teleoperator is Input-to-State Stable from human operator and environment inputs to some synchronization signals. Simulations show the effectiveness of the proposed controllers.**

I. Introduction

A bilateral teleoperator is composed of five elements: a *human operator* that exerts torques on a *local manipulator*, which is connected through a *communication channel* to a *remote manipulator* that interacts with an *environment*. Such interaction is then reflected back to the operator (Fig. 1). The communication channel often imposes time-delays, and such delays can produce instabilities in the overall system. A major breakthrough in the problem of control of these systems, with guaranteed stability properties, was the use of scattering signals to transform the transmission delays into a passive transmission line. Under the reasonable assumption that the human operator and the contact environment define passive (force to velocity) maps, stability of the overall system is then ensured [1], [2], [3]. However, most of the scattering-based approaches cannot ensure accurate position tracking. PD–like schemes that overcome this obstacle without scattering, have been reported in [4], [5]. However, in order to ensure asymptotical stability the PD–like schemes need exact knowledge of the gravity forces.

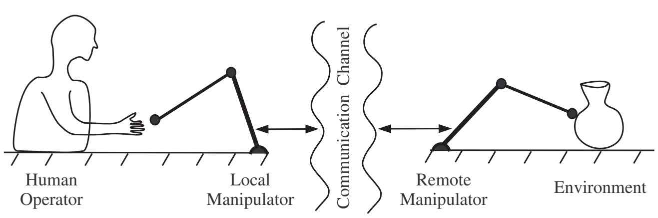

Fig. 1. Bilateral teleoperator

Recently, [6] proposed to formulate the teleoperation problem in terms of synchronization, which also avoids the scattering transformation. An adaptive version of this scheme, which aims at synchronizing the local and remote positions and velocities, is proposed in [7]. In [8], the synchronization of Lagrangian systems to a predefined trajectory is solved using contraction analysis.

This paper proposes two different adaptive controllers that provide asymptotic convergence of velocity and position errors to zero, independent of the constant time-delays. On one hand, the first of the proposed controllers, needs acceleration measurements, and it can be proved that the corresponding dynamics are strictly output passive. The second controller does not rely on acceleration measurements, but instead injects damping to provide asymptotic stability. In general, convergence is faster using acceleration measurements than using the velocity based controller. This paper also proves that the teleoperator is Input-to-State Stable (ISS), meaning that with bounded human operator and environment forces, the states remain bounded, and if the human operator and the environment do not exert any forces, the states asymptotically converge to zero.

A. Notation

The following notation is used throughout this paper. Capital letters are used for matrices and lower case letters for vectors. $\mathbb{R} := (-\infty, \infty)$, $\mathbb{R}_{>0} := (0, \infty)$, $\mathbb{R}_{\geq 0} := [0, \infty)$. $\lambda_m\{\mathbf{A}\}$ and $\lambda_M\{\mathbf{A}\}$ represent the minimum and maximum eigenvalues of matrix $\mathbf{A}$, respectively. $|\mathbf{x}|$ stands for the standard Euclidean norm of vector $\mathbf{x}$. For any function $\mathbf{f} : \mathbb{R}_{\geq 0} \to \mathbb{R}^n$, the $\mathcal{L}_\infty$-norm is defined as $\|\mathbf{f}\|_\infty = \sup_{t\in[0,\infty)} |\mathbf{f}(t)|$, and the $\mathcal{L}_2$-norm as $\|\mathbf{f}\|_2^2 = \int_0^\infty |\mathbf{f}(t)|^2 dt$. The $\mathcal{L}_\infty$ and $\mathcal{L}_2$ spaces are defined as the sets $\{\mathbf{f} : \mathbb{R}_{\geq 0} \to \mathbb{R}^n : \|\mathbf{f}\|_\infty < \infty\}$ and $\{\mathbf{f} : \mathbb{R}_{\geq 0} \to \mathbb{R}^n : \|\mathbf{f}\|_2 < \infty\}$, respectively. When clear from the context, the argument of signals and operators is removed.

II. Teleoperator Dynamics

The dynamic behavior of a n-Degrees Of Freedom (DOF) manipulator can be derived from the Euler-Lagrange equations of motion

$$L(\mathbf{q}, \dot{\mathbf{q}}) = \frac{1}{2}\dot{\mathbf{q}}^\top \mathbf{M}(\mathbf{q})\dot{\mathbf{q}} - U(\mathbf{q}); \qquad \frac{d}{dt}\frac{\partial L}{\partial \dot{\mathbf{q}}} - \frac{\partial L}{\partial \mathbf{q}} = \boldsymbol{\tau}$$

where $L(\mathbf{q}, \dot{\mathbf{q}})$ is the so-called Lagrangian and $U(\mathbf{q})$ is the potential energy. $\dot{\mathbf{q}}, \mathbf{q} \in \mathbb{R}^n$ are the joint velocities and positions, respectively, and $\mathbf{M}(\mathbf{q}) \in \mathbb{R}^{n\times n}$ is the inertia matrix. In compact form, these equations can be written as

$$\mathbf{M}(\mathbf{q})\ddot{\mathbf{q}} + \mathbf{C}(\mathbf{q}, \dot{\mathbf{q}})\dot{\mathbf{q}} + \mathbf{g}(\mathbf{q}) = \boldsymbol{\tau} \tag{1}$$

[1] Electronics and Computer Science Division. CUCEI. University of Guadalajara (UDG). Guadalajara, Mexico.

[2] Institute of Industrial and Control Engineering (IOC). Technical University of Catalonia (UPC). Barcelona, Spain.

[3] Laboratoire des Signaux et Systèmes. SUPÉLEC. Gif-sur-Yvette, France.

E-mail: emmanuel.nuno@cucei.udg.mx, luis.basanez@upc.edu, ortega@lss.supelec.fr, guillermo.obregon@cucei.udg.mx

where $\ddot{\mathbf{q}} \in \mathbb{R}^n$ is the joint acceleration vector; $\mathbf{C}(\mathbf{q},\dot{\mathbf{q}}) \in \mathbb{R}^{n\times n}$ is the Coriolis and centrifugal effects matriz; $\mathbf{g}(\mathbf{q}) = \frac{\partial U(\mathbf{q})}{\partial \mathbf{q}} \in \mathbb{R}^n$ is the gravitational force vector, and $\boldsymbol{\tau} \in \mathbb{R}^n$ is a generalized force vector.

The dynamical system (1) possesses some important and well–known properties [9], [10].

P1. $0 < \lambda_m\{\mathbf{M}(\mathbf{q})\}\mathbf{I} \leq \mathbf{M}(\mathbf{q}) \leq \lambda_M\{\mathbf{M}(\mathbf{q})\}\mathbf{I} < \infty$ and $\mathbf{M}(\mathbf{q}) = \mathbf{M}^\top(\mathbf{q})$

P2. $\forall \mathbf{x} \neq \mathbf{0} \in \mathbb{R}^n : \ \mathbf{x}^\top[\dot{\mathbf{M}}(\mathbf{q}) - 2\mathbf{C}(\mathbf{q},\dot{\mathbf{q}})]\mathbf{x} = 0$

P3. $\exists k_c \in \mathbb{R}_{>0} : \ |\mathbf{C}(\mathbf{q},\dot{\mathbf{q}})\dot{\mathbf{q}}| \leq k_c|\dot{\mathbf{q}}|^2$.

P4. $\mathbf{M}(\mathbf{q})\ddot{\mathbf{q}} + \mathbf{C}(\mathbf{q},\dot{\mathbf{q}})\dot{\mathbf{q}} + \mathbf{g}(\mathbf{q}) = \mathbf{Y}(\mathbf{q},\dot{\mathbf{q}},\ddot{\mathbf{q}})\boldsymbol{\theta}$

where, in P4, $\mathbf{Y}(\mathbf{q},\dot{\mathbf{q}},\ddot{\mathbf{q}}) \in \mathbb{R}^{n\times p}$ is a matrix of known functions and $\boldsymbol{\theta} \in \mathbb{R}^p$ is a constant vector with the manipulator physical parameters (link masses, moments of inertia, etc.).

Remark 1: It is widely known that dynamics (1) define a passive map $\boldsymbol{\tau} \mapsto \dot{\mathbf{q}}$ [11]. This is proved using the storage function $V = \frac{1}{2}\dot{\mathbf{q}}^\top\mathbf{M}(\mathbf{q})\dot{\mathbf{q}} + U(\mathbf{q})$, yielding $\dot{V} = \dot{\mathbf{q}}^\top\boldsymbol{\tau}$. Hence, after integration, $\int_0^t \dot{\mathbf{q}}^\top\boldsymbol{\tau}d\tau \geq -V(0)$.

A bilateral teleoperator can be modeled as a pair of n-DOF manipulators with serial links of the form (1). Neglecting friction, its nonlinear dynamics, together with the human operator and environment interactions, are given by

$$\begin{aligned} \mathbf{M}_l(\mathbf{q}_l)\ddot{\mathbf{q}}_l + \mathbf{C}_l(\mathbf{q}_l,\dot{\mathbf{q}}_l)\dot{\mathbf{q}}_l + \mathbf{g}_l(\mathbf{q}_l) &= \boldsymbol{\tau}_h - \boldsymbol{\tau}_l \\ \mathbf{M}_r(\mathbf{q}_r)\ddot{\mathbf{q}}_r + \mathbf{C}_r(\mathbf{q}_r,\dot{\mathbf{q}}_r)\dot{\mathbf{q}}_r + \mathbf{g}_r(\mathbf{q}_r) &= \boldsymbol{\tau}_r - \boldsymbol{\tau}_e, \end{aligned} \tag{2}$$

where $\boldsymbol{\tau}_i \in \mathbb{R}^n$ are the control signals, and $\boldsymbol{\tau}_h, \boldsymbol{\tau}_e \in \mathbb{R}^n$ are the forces exerted by the human and the environment, respectively. The subscript i takes the values l and r for local and remote robot manipulators. It is assumed that the manipulators contain fully actuated revolute joints.

III. Position Tracking

Let $\mathbf{e}_i \in \mathbb{R}^n$ denote the position error, defined, for constant time-delays T_i in the forward and backward paths, as

$$\mathbf{e}_l = \mathbf{q}_l - \mathbf{q}_r(t - T_r); \quad \mathbf{e}_r = \mathbf{q}_r - \mathbf{q}_l(t - T_l). \tag{3}$$

The objective of the controllers in this paper is to drive the position and velocity errors, $\mathbf{e}_i, \dot{\mathbf{e}}_i$, to zero independently of the constant time-delays T_i and without using the ubiquitous scattering transformation.

A. Controller Using Acceleration Measurements

Let us start by defining a *synchronizing signal*, that can be seen as a direct application of the Slotine-Li variable where, instead of a common desired trajectory, the velocity and position errors between the local and the remote manipulators are employed as

$$\mathbf{r}_i = \dot{\mathbf{e}}_i + \boldsymbol{\lambda}\mathbf{e}_i, \tag{4}$$

where $\boldsymbol{\lambda}$ is a diagonal positive definite matrix.

The proposed controllers are[1]

$$\begin{aligned} \boldsymbol{\tau}_l &= -\hat{\mathbf{M}}_l(\ddot{\mathbf{q}}_{r,d} - \boldsymbol{\lambda}\dot{\mathbf{e}}_l) - \hat{\mathbf{C}}_l(\dot{\mathbf{q}}_{r,d} - \boldsymbol{\lambda}\mathbf{e}_l) - \hat{\mathbf{g}}_l + \mathbf{K}_l\mathbf{r}_l \\ \boldsymbol{\tau}_r &= \hat{\mathbf{M}}_r(\ddot{\mathbf{q}}_{l,d} - \boldsymbol{\lambda}\dot{\mathbf{e}}_r) + \hat{\mathbf{C}}_r(\dot{\mathbf{q}}_{l,d} - \boldsymbol{\lambda}\mathbf{e}_r) + \hat{\mathbf{g}}_r - \mathbf{K}_r\mathbf{r}_r, \end{aligned}$$

[1] In order to shorten the equations we will add the subindex d to denote a delayed signal, e.g., $\mathbf{q}_{r,d} = \mathbf{q}_r(t - T_r)$ or $\dot{\mathbf{q}}_{l,d} = \dot{\mathbf{q}}_l(t - T_l)$.

where $\mathbf{K}_r \in \mathbb{R}^{n\times n}$ are symmetric and positive definite gain matrices, $\hat{\mathbf{M}}_i, \hat{\mathbf{C}}_i, \hat{\mathbf{g}}_i$ are the estimates of the inertia and Coriolis matrices, and the gravity forces, respectively.

From P4, these controllers can be also written as

$$\begin{aligned} \boldsymbol{\tau}_l &= -\mathbf{Y}_l(\mathbf{q}_l,\dot{\mathbf{q}}_l,\mathbf{e}_l,\dot{\mathbf{e}}_l,\ddot{\mathbf{q}}_{r,d},\dot{\mathbf{q}}_{r,d})\hat{\boldsymbol{\theta}}_l + \mathbf{K}_l\mathbf{r}_l \\ \boldsymbol{\tau}_r &= \mathbf{Y}_r(\mathbf{q}_r,\dot{\mathbf{q}}_r,\mathbf{e}_r,\dot{\mathbf{e}}_r,\ddot{\mathbf{q}}_{l,d},\dot{\mathbf{q}}_{l,d})\hat{\boldsymbol{\theta}}_r - \mathbf{K}_r\mathbf{r}_r \end{aligned} \tag{5}$$

where $\mathbf{Y}_i$ are the regressor matrices of known functions, $\hat{\boldsymbol{\theta}}_i$ are the physical estimated parameters. Fig. 2 shows the schematics of the adaptive controller for one manipulator, that can be either in the local or in the remote site.

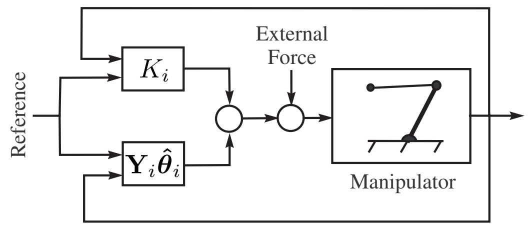

Fig. 2. Adaptive control for one manipulator.

Note that for the known parameter case

$$\mathbf{Y}_l\boldsymbol{\theta}_l = \mathbf{M}_l(\mathbf{q}_l)(\ddot{\mathbf{q}}_{r,d} - \boldsymbol{\lambda}\dot{\mathbf{e}}_l) + \mathbf{C}_l(\mathbf{q}_l,\dot{\mathbf{q}}_l)(\dot{\mathbf{q}}_{r,d} - \boldsymbol{\lambda}\mathbf{e}_l) + \mathbf{g}_l(\mathbf{q}_l).$$

Substituting the controllers (5) in the teleoperator dynamics (2) and using (4), yields

$$\begin{aligned} \mathbf{M}_l(\mathbf{q}_l)\dot{\mathbf{r}}_l + \mathbf{C}_l(\mathbf{q}_l,\dot{\mathbf{q}}_l)\mathbf{r}_l + \mathbf{K}_l\mathbf{r}_l &= \mathbf{Y}_l\tilde{\boldsymbol{\theta}}_l + \boldsymbol{\tau}_h \\ \mathbf{M}_r(\mathbf{q}_r)\dot{\mathbf{r}}_r + \mathbf{C}_r(\mathbf{q}_r,\dot{\mathbf{q}}_r)\mathbf{r}_r + \mathbf{K}_r\mathbf{r}_r &= \mathbf{Y}_r\tilde{\boldsymbol{\theta}}_r - \boldsymbol{\tau}_e, \end{aligned} \tag{6}$$

where $\tilde{\boldsymbol{\theta}}_i = \hat{\boldsymbol{\theta}}_i - \boldsymbol{\theta}_i$ are the errors between the estimation and the unknown real parameters.

Without the influence of the human operator and the environment, the differential equations (6) can be written as

$$\mathbf{M}_i(\mathbf{q}_i)\dot{\mathbf{r}}_i + \mathbf{C}_i(\mathbf{q}_i,\dot{\mathbf{q}}_i)\mathbf{r}_i + \mathbf{K}_i\mathbf{r}_i = \mathbf{Y}_i\tilde{\boldsymbol{\theta}}_i = \boldsymbol{\Psi}_i \tag{7}$$

Remark 2: As first shown in [12], (7) defines an output strictly passive map $\boldsymbol{\Psi}_i \mapsto \mathbf{r}_i$. Consider $V_i = \frac{1}{2}\mathbf{r}_i^\top\mathbf{M}_i(\mathbf{q}_i)\mathbf{r}_i$ as a storage function. After evaluating V_i along (7), it can be seen that $\dot{V}_i \leq \mathbf{r}_i^\top\boldsymbol{\Psi}_i - \lambda_m\{\mathbf{K}_i\}|\mathbf{r}_i|^2$. Integrating from 0 to t, and due to $V_i > 0$, yields

$$\int_0^t \mathbf{r}_i^\top\boldsymbol{\Psi}_i d\sigma \geq \lambda_m\{\mathbf{K}_i\}\|\mathbf{r}_i\|_2^2 - V_i(0).$$

This suggests that, if it is possible to generate a passive map $-\mathbf{r}_i \mapsto \boldsymbol{\Psi}_i$, then $\mathbf{r}_i \in \mathcal{L}_2$. This is due to the well-known passivity theorem that ensures $\mathcal{L}_2$-stability of the feedback interconnection of a passive and an output strictly passive map [13].

Proposition 1: Consider (7). Suppose the map $-\mathbf{r}_i \mapsto \boldsymbol{\Psi}_i$ is passive, such that

$$-\int_0^t \mathbf{r}_i^\top\boldsymbol{\Psi}_i d\sigma + \kappa_i \geq 0$$

for all t and some $\kappa_i \geq 0$. Then $|\mathbf{e}_i| \to 0$ as $t \to \infty$. If additionally $\boldsymbol{\Psi}_i \in \mathcal{L}_\infty$ then, independently of the magnitude of the constant time-delays T_i, $|\dot{\mathbf{e}}_i| \to |\mathbf{r}_i| \to 0$ as $t \to \infty$.

Proof: Consider the following positive semi-definite Lyapunov-Razumikhin functional

$$V=\sum_{i\in\{l,r\}}\left[\frac{1}{2}\mathbf{r}_i^\top\mathbf{M}_i(\mathbf{q}_i)\mathbf{r}_i-\int_0^t\mathbf{r}_i^\top\boldsymbol{\Psi}_i d\sigma+\kappa_i\right].$$

Differentiating V along the trajectories of (7) and using P2 yields

$$\dot V=-\sum_{i\in\{l,r\}}\mathbf{r}_i^\top\mathbf{K}_i\mathbf{r}_i\leq 0$$

Due to $V\geq 0$ and $\dot V\leq 0$, $\mathbf{r}_i\in\mathcal{L}_2\cap\mathcal{L}_\infty$. From (4) $\mathbf{E}_i(s)=(s\mathbf{I}+\boldsymbol{\lambda})^{-1}\mathbf{R}_i(s)$, where s is the Laplace variable, hence from Lemma 1 —stated in the Appendix, it follows that $\mathbf{e}_i\in\mathcal{L}_2\cap\mathcal{L}_\infty$, $\dot{\mathbf{e}}_i\in\mathcal{L}_2$, and $|\mathbf{e}_i|\to 0$ as $t\to\infty$. Now, if $\boldsymbol{\Psi}_i\in\mathcal{L}_\infty$, from (7) and P1, it can be concluded that $\dot{\mathbf{r}}_i\in\mathcal{L}_\infty$ and, by Barbălat's Lemma, $|\mathbf{r}_i|\to 0$, consequently $|\dot{\mathbf{e}}_i|\to 0$. ■

B. Controller Without Acceleration Measurements

In this case, the *synchronizing signal* is given by

$$\boldsymbol{\epsilon}_i=\dot{\mathbf{q}}_i+\boldsymbol{\lambda}\mathbf{e}_i. \quad (8)$$

The controllers that do not depend on acceleration measurements are

$$\begin{aligned}\boldsymbol{\tau}_l &= \hat{\mathbf{M}}_l\boldsymbol{\lambda}\dot{\mathbf{e}}_l+\hat{\mathbf{C}}_l\boldsymbol{\lambda}\mathbf{e}_l-\hat{\mathbf{g}}_l+\mathbf{K}_l\boldsymbol{\epsilon}_l+\mathbf{B}\dot{\mathbf{e}}_l\\ \boldsymbol{\tau}_r &= -\hat{\mathbf{M}}_r\boldsymbol{\lambda}\dot{\mathbf{e}}_r-\hat{\mathbf{C}}_r\boldsymbol{\lambda}\mathbf{e}_r+\hat{\mathbf{g}}_r-\mathbf{K}_r\boldsymbol{\epsilon}_r-\mathbf{B}\dot{\mathbf{e}}_r,\end{aligned}$$

thus,

$$\begin{aligned}\boldsymbol{\tau}_l &= -\mathbf{Y}_l(\mathbf{q}_l,\dot{\mathbf{q}}_l,\mathbf{e}_l,\dot{\mathbf{e}}_l)\hat{\boldsymbol{\theta}}_l+\mathbf{K}_l\boldsymbol{\epsilon}_l+\mathbf{B}\dot{\mathbf{e}}_l\\ \boldsymbol{\tau}_r &= \mathbf{Y}_r(\mathbf{q}_r,\dot{\mathbf{q}}_r,\mathbf{e}_r,\dot{\mathbf{e}}_r)\hat{\boldsymbol{\theta}}_r-\mathbf{K}_r\boldsymbol{\epsilon}_r-\mathbf{B}\dot{\mathbf{e}}_r. \quad (9)\end{aligned}$$

where $\mathbf{K}_i=\mathbf{K}_i^\top>0$ and $\mathbf{B}>0$ is diagonal[2]. Using (8) and (9) we can write (2), with $\boldsymbol{\tau}_h=\boldsymbol{\tau}_e=\mathbf{0}$, as

$$\mathbf{M}_i(\mathbf{q}_i)\dot{\boldsymbol{\epsilon}}_i+\mathbf{C}_i(\mathbf{q}_i,\dot{\mathbf{q}}_i)\boldsymbol{\epsilon}_i+\mathbf{K}_i\boldsymbol{\epsilon}_i+\mathbf{B}\dot{\mathbf{e}}_i=\mathbf{Y}_i\tilde{\boldsymbol{\theta}}_i=\boldsymbol{\Phi}_i \quad (10)$$

Remark 3: Removing $\mathbf{B}\dot{\mathbf{e}}_i$ from (10), yields

$$\mathbf{M}_i(\mathbf{q}_i)\dot{\boldsymbol{\epsilon}}_i+\mathbf{C}_i(\mathbf{q}_i,\dot{\mathbf{q}}_i)\boldsymbol{\epsilon}_i+\mathbf{K}_i\boldsymbol{\epsilon}_i=\mathbf{Y}_i\tilde{\boldsymbol{\theta}}_i=\boldsymbol{\Phi}_i$$

which is similar to (7). Moreover, as in Proposition 1, these dynamics provide a strict output map from $\boldsymbol{\Phi}_i$ to $\boldsymbol{\epsilon}_i$. The result is that $\int_0^t\boldsymbol{\epsilon}_i^\top\boldsymbol{\Phi}_i d\sigma\geq\lambda_m\{\mathbf{K}_i\}\|\boldsymbol{\epsilon}_i\|_2^2-V_i(0)$, for $V_i(0)\geq 0$. However, from the function

$$V=\frac{1}{2}\sum_{i\in\{l,r\}}\left[\boldsymbol{\epsilon}_i^\top\mathbf{M}_i(\mathbf{q}_i)\boldsymbol{\epsilon}_i-\int_0^t\boldsymbol{\epsilon}_i^\top\boldsymbol{\Phi}_i d\sigma+\kappa_i\right]$$

it can only be concluded that $\boldsymbol{\epsilon}_i\in\mathcal{L}_2\cap\mathcal{L}_\infty$, and because of (8), Lemma 1 cannot be invoked to show convergence of position error. This is why $\mathbf{B}\dot{\mathbf{e}}_i$ must be included in the controllers.

Proposition 2: Consider (10). Suppose the map $-\boldsymbol{\epsilon}_i\mapsto\boldsymbol{\Phi}_i$ is passive, such that

$$-\int_0^t\boldsymbol{\epsilon}_i^\top\boldsymbol{\Phi}_i d\sigma+\kappa_i\geq 0,$$

for all t and some $\kappa_i\geq 0$. Then $\boldsymbol{\epsilon}_i\in\mathcal{L}_2\cap\mathcal{L}_\infty$ and $\mathbf{e}_i,\dot{\mathbf{q}}_i\in\mathcal{L}_\infty$. If additionally, $\boldsymbol{\Phi}_i\in\mathcal{L}_\infty$, then, for any constant time-delays T_i, position errors and velocities asymptotically converge to zero.

Proof: Consider the following Lyapunov-Krasovskiĭ functional

$$\begin{aligned}V &= \frac{1}{2}\sum_{i\in\{l,r\}}\left[\boldsymbol{\epsilon}_i^\top\mathbf{M}_i\boldsymbol{\epsilon}_i+\mathbf{e}_i^\top\boldsymbol{\lambda}\mathbf{B}\mathbf{e}_i+\int_{t-T_i}^t\dot{\mathbf{q}}_i^\top\mathbf{B}\dot{\mathbf{q}}_i d\sigma\right]+\\ &+\sum_{i\in\{l,r\}}\left[\kappa_i-\int_0^t\boldsymbol{\epsilon}_i^\top\boldsymbol{\Phi}_i d\sigma\right].\end{aligned}$$

V is positive definite and radially unbounded in $\boldsymbol{\epsilon}_i,\mathbf{e}_i$. Its time-derivative $\dot V$ along (10), using P2, is given by

$$\sum_{i\in\{l,r\}}\left[\dot{\mathbf{q}}_i^\top\mathbf{B}\dot{\mathbf{e}}_i-\boldsymbol{\epsilon}_i^\top\mathbf{K}_i\boldsymbol{\epsilon}_i+\frac{1}{2}\dot{\mathbf{q}}_i^\top\mathbf{B}\dot{\mathbf{q}}_i-\frac{1}{2}\dot{\mathbf{q}}_i^\top(t-T_i)\mathbf{B}\dot{\mathbf{q}}_i(t-T_i)\right].$$

Notice that, for $i=l$, $\dot{\mathbf{q}}_l^\top\mathbf{B}\dot{\mathbf{e}}_l=\dot{\mathbf{q}}_l^\top\mathbf{B}(\dot{\mathbf{q}}_r(t-T)-\dot{\mathbf{q}}_l)$. Hence, when $i=r$ and gathering the crossed terms $-\frac{1}{2}[\dot{\mathbf{q}}_l^\top\mathbf{B}\dot{\mathbf{q}}_l-2\dot{\mathbf{q}}_l^\top\mathbf{B}\dot{\mathbf{q}}_r(t-T)+\dot{\mathbf{q}}_r^\top(t-T)\mathbf{B}\dot{\mathbf{q}}_r(t-T)]$, yields

$$\dot V=-\sum_{i\in\{l,r\}}\left[\boldsymbol{\epsilon}_i^\top\mathbf{K}_i\boldsymbol{\epsilon}_i+\frac{1}{2}\dot{\mathbf{e}}_i^\top\mathbf{B}\dot{\mathbf{e}}_i\right].$$

Due to $V\geq 0$ and $\dot V\leq 0$, $\boldsymbol{\epsilon}_i,\dot{\mathbf{e}}_i\in\mathcal{L}_2$ and $\boldsymbol{\epsilon}_i,\mathbf{e}_i\in\mathcal{L}_\infty$. Using (8) it can be shown that $\dot{\mathbf{q}}_i\in\mathcal{L}_\infty$, implying that $\dot{\mathbf{e}}_i\in\mathcal{L}_\infty$. From (10), using P1 together with boundedness of $\boldsymbol{\Phi}_i$, it can be shown that $\dot{\boldsymbol{\epsilon}}_i\in\mathcal{L}_\infty$. Hence, with $\boldsymbol{\epsilon}_i\in\mathcal{L}_\infty\cap\mathcal{L}_2$, $\dot{\boldsymbol{\epsilon}}_i\in\mathcal{L}_\infty$ it is proved that $|\boldsymbol{\epsilon}_i|\to 0$.

$\dot{\boldsymbol{\epsilon}}_i,\dot{\mathbf{e}}_i\in\mathcal{L}_\infty$ imply that $\ddot{\mathbf{q}}_i\in\mathcal{L}_\infty$, hence $\ddot{\mathbf{e}}_i\in\mathcal{L}_\infty$. This last, and the fact that $\dot{\mathbf{e}}_i\in\mathcal{L}_\infty\cap\mathcal{L}_2$ prove that $|\dot{\mathbf{e}}_i|\to 0$.

Now, $\mathbf{e}_i,\dot{\mathbf{e}}_i,\ddot{\mathbf{e}}_i\in\mathcal{L}_\infty$ and $|\dot{\mathbf{e}}_i|\to 0$ imply that $\lim_{t\to\infty}\int_0^t\dot{\mathbf{e}}_i d\sigma=\mathbf{e}_i-\mathbf{e}_i(0)=k_i<\infty$. On the other hand,

$$\lim_{t\to\infty}|\boldsymbol{\epsilon}_i|=\lim_{t\to\infty}|\dot{\mathbf{q}}_i+\boldsymbol{\lambda}\mathbf{e}_i|=\lim_{t\to\infty}|\dot{\mathbf{q}}_i-\boldsymbol{\lambda}(k_i+\mathbf{e}_i(0))|=0$$

imply that when $t\to\infty$, $\dot{\mathbf{q}}_i\to\boldsymbol{\lambda}(k_i+\mathbf{e}_i(0))$ that is constant. This and $|\dot{\mathbf{e}}_i|\to 0$ ensure that $|\dot{\mathbf{q}}_i|\to|\dot{\mathbf{q}}_c|$, for $\dot{\mathbf{q}}_c$ any constant vector, and $\mathbf{q}_l-\mathbf{q}_r(t-T)=\mathbf{q}_l-\mathbf{q}_r$. Thus, in the limit, $\boldsymbol{\epsilon}_l=\dot{\mathbf{q}}_c+\boldsymbol{\lambda}\mathbf{e}_l=\dot{\mathbf{q}}_c-\boldsymbol{\lambda}\mathbf{e}_r$. Hence $\boldsymbol{\epsilon}_l+\boldsymbol{\epsilon}_r=2\dot{\mathbf{q}}_c$, the fact that $|\boldsymbol{\epsilon}_i|\to 0$ implies that $\dot{\mathbf{q}}_c=\mathbf{0}$. Thus, $|\dot{\mathbf{q}}_i|\to|\mathbf{e}_i|\to 0$. This completes the proof. ■

C. Parameter Estimation

Let us now show that there exists a passive map $-\mathbf{r}_i\mapsto\boldsymbol{\Psi}_i$ and that $\boldsymbol{\Psi}_i\in\mathcal{L}_\infty$, such that the assumptions in Proposition 1 hold. Define the following parameter estimation law

$$\dot{\hat{\boldsymbol{\theta}}}_i=-\boldsymbol{\Gamma}_i\mathbf{Y}_i^\top\mathbf{r}_i, \quad (11)$$

where $\boldsymbol{\Gamma}_i=\boldsymbol{\Gamma}_i^\top>0$ and $\mathbf{Y}_i$ is defined as in (5). Note that $\dot{\tilde{\boldsymbol{\theta}}}_i=\dot{\hat{\boldsymbol{\theta}}}_i$. Thus,

$$\mathbf{r}_i^\top\boldsymbol{\Psi}_i=\mathbf{r}_i^\top\mathbf{Y}_i\tilde{\boldsymbol{\theta}}_i=-\tilde{\boldsymbol{\theta}}_i^\top\boldsymbol{\Gamma}_i^{-1}\dot{\tilde{\boldsymbol{\theta}}}_i.$$

Hence, we have that

$$-\int_0^t\mathbf{r}_i^\top\boldsymbol{\Psi}_i d\sigma=\int_0^t\tilde{\boldsymbol{\theta}}_i^\top\boldsymbol{\Gamma}_i^{-1}\dot{\tilde{\boldsymbol{\theta}}}_i d\sigma=\frac{1}{2}\tilde{\boldsymbol{\theta}}_i^\top\boldsymbol{\Gamma}_i^{-1}\tilde{\boldsymbol{\theta}}_i-\kappa_i\geq-\kappa_i$$

[2] $\mathbf{B}$ is chosen diagonal in order to ensure that the product $\boldsymbol{\lambda}\mathbf{B}$, used in the proof of the stability, is positive definite.

where $\kappa_i = \frac{1}{2}\tilde{\boldsymbol{\theta}}_i^\top(0)\boldsymbol{\Gamma}_i^{-1}\tilde{\boldsymbol{\theta}}_i(0)$. Thus, (11) provides a passive map $-\mathbf{r}_i \mapsto \boldsymbol{\Psi}_i$.

Now, substituting in V, in the proof of Proposition 1, the positive semi-definite terms

$$-\int_0^t \boldsymbol{\epsilon}_i^\top \boldsymbol{\Psi}_i d\sigma + \kappa_i = \frac{1}{2}\tilde{\boldsymbol{\theta}}_i^\top \boldsymbol{\Gamma}_i^{-1}\tilde{\boldsymbol{\theta}}_i$$

one can conclude that, because $V \in \mathcal{L}_\infty$, $\tilde{\boldsymbol{\theta}}_i \in \mathcal{L}_\infty$. The proof that $\boldsymbol{\Psi}_i = \mathbf{Y}_i\tilde{\boldsymbol{\theta}}_i \in \mathcal{L}_\infty$ is established with the fact that $\mathbf{r}_i, \tilde{\boldsymbol{\theta}}_i \in \mathcal{L}_\infty$.

Remark 4: The assumptions in Proposition 2 also hold. The proof is done using the previous procedure, in which the map $-\boldsymbol{\epsilon}_i \mapsto \boldsymbol{\Phi}_i$ is proved passive and $\boldsymbol{\Phi}_i \in \mathcal{L}_\infty$ with the adaptation law $\dot{\hat{\boldsymbol{\theta}}}_i = -\boldsymbol{\Gamma}_i\mathbf{Y}_i^\top\boldsymbol{\epsilon}_i$ and $\mathbf{Y}_i$ defined as in (9).

D. Input-to-State Stability

When the human operator and the environment exert forces on the local and remote manipulators, respectively, the teleoperator exhibits an Input-to-State Stable (ISS) behavior, from inputs $\boldsymbol{\tau}_h, \boldsymbol{\tau}_e$ to states $\mathbf{r}_i$. This means that the states remain bounded when the inputs are bounded, and, as proved in the previous sections, the states asymptotically converge to zero when inputs are zero.

Proposition 3: Consider the system (4) and (6) with the parameter update law (11). Then, for any constant time-delays T_i, the teleoperator is ISS with states $\mathbf{r}_i$ and inputs $\boldsymbol{\tau}_h, \boldsymbol{\tau}_e$.

Proof: Consider the following Lyapunov-Razumikhin functional

$$V = \frac{1}{2}\sum_{i\in\{l,r\}}\left[\mathbf{r}_i^\top\mathbf{M}_i(\mathbf{q}_i)\mathbf{r}_i + \tilde{\boldsymbol{\theta}}_i^\top\boldsymbol{\Gamma}_i^{-1}\tilde{\boldsymbol{\theta}}_i\right].$$

This functional is positive definite and radially unbounded in $\mathbf{r}_i$ and $\tilde{\boldsymbol{\theta}}_i$. It can be clearly seen, using P1, that there exist $\nu_1, \nu_2 \in \mathbb{R}_{>0}$ such that

$$\nu_1(|\mathbf{r}_l|^2 + |\tilde{\boldsymbol{\theta}}_l|^2) \le V \le \nu_2(|\mathbf{r}_l|^2 + |\tilde{\boldsymbol{\theta}}_l|^2).$$

The time derivative of V along the trajectories (6) and (11) is given by

$$\dot{V} = -\mathbf{r}_l^\top(\mathbf{K}_l\mathbf{r}_l - \boldsymbol{\tau}_h) - \mathbf{r}_r^\top(\mathbf{K}_r\mathbf{r}_r + \boldsymbol{\tau}_e).$$

It can be easily proved, using Young's inequality, that there exist positive constants α_j such that

$$\dot{V} \le -\alpha_l\|\mathbf{r}_l\|^2 - \alpha_r\|\mathbf{r}_r\|^2 + \alpha_h\|\boldsymbol{\tau}_h\|^2 + \alpha_e\|\boldsymbol{\tau}_e\|^2$$

Hence, the teleoperator is ISS with states $\mathbf{r}_i$ and inputs $\boldsymbol{\tau}_h, \boldsymbol{\tau}_e$ [14]. ■

Remark 5: Similar ISS conclusions can be drawn for the teleoperator (2) controlled by (9) with the parameter update law $\dot{\hat{\boldsymbol{\theta}}}_i = -\boldsymbol{\Gamma}_i\mathbf{Y}_i^\top\boldsymbol{\epsilon}_i$. In this case, it is proved that the teleoperator is ISS from inputs $\boldsymbol{\tau}_h, \boldsymbol{\tau}_e$ to states $\boldsymbol{\epsilon}_i, \mathbf{e}_i$ [15]. The proposed Lyapunov-Razumikhin functional, for two positive α_i, is given by

$$V = \frac{1}{2}\sum_{i\in\{l,r\}}\left[\boldsymbol{\epsilon}_i^\top\mathbf{M}_i(\mathbf{q}_i)\boldsymbol{\epsilon}_i + \tilde{\boldsymbol{\theta}}_i^\top\boldsymbol{\Gamma}_i^{-1}\tilde{\boldsymbol{\theta}}_i + \alpha_i|\mathbf{e}_i|^2\right].$$

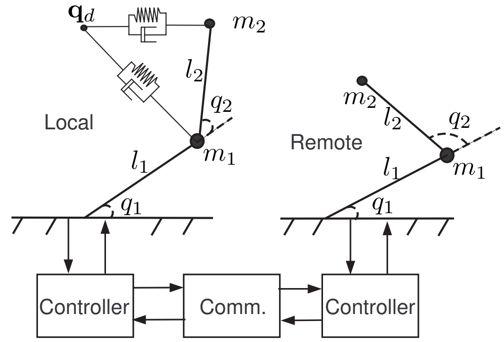

Fig. 3. Simulations scheme.

IV. Simulations

To show the effectiveness of the proposed schemes, some simulations, in which the local and remote manipulators are modeled as a pair of 2 DOF serial links with revolute joints (cf. Fig. 3), are presented. Their corresponding nonlinear dynamics are modeled by (1). In what follows $\alpha_i := l_{2_i}^2 m_{2_i} + l_{1_i}^2(m_{1_i} + m_{2_i})$, $\beta_i := l_{1_i}l_{2_i}m_{2_i}$ and $\delta_i := l_{2_i}^2 m_{2_i}$. The inertia matrices $\mathbf{M}_i(\mathbf{q}_i)$ are given by

$$\mathbf{M}_i(\mathbf{q}_i) = \begin{bmatrix} \alpha_i + 2\beta_i \mathrm{c}_{2_i} & \delta_i + \beta_i\mathrm{c}_{2_i} \\ \delta_i + \beta_i\mathrm{c}_{2_i} & \delta_i \end{bmatrix}.$$

c_{2_i} is the short notation for $\cos(q_{2_i})$. q_{k_i} is the articular position of link k of manipulator i, with $k \in \{1,2\}$. The Coriolis and centrifugal effects are modeled by

$$\mathbf{C}_i(\mathbf{q}_i, \dot{\mathbf{q}}_i) = \begin{bmatrix} -2\beta_i\mathrm{s}_{2_i}\dot{q}_{2_i} & -\beta_i\mathrm{s}_{2_i}\dot{q}_{2_i} \\ \beta_i\mathrm{s}_{2_i}\dot{q}_{1_i} & 0 \end{bmatrix}.$$

s_{2_i} is the short notation for $\sin(q_{2_i})$. $\dot{q}_{1_i}$ and $\dot{q}_{2_i}$ are the respective revolute velocities of the two links. The gravity forces $\mathbf{g}_i(\mathbf{q}_i)$ for each manipulator are represented by

$$\mathbf{g}_i(\mathbf{q}_i) = \begin{bmatrix} \frac{1}{l_{2_i}}g\delta_i\mathrm{c}_{12_i} + \frac{1}{l_{1_i}}(\alpha_i - \delta_i)\mathrm{c}_{1_i} \\ \frac{1}{l_{2_i}}g\delta_i\mathrm{c}_{12_i} \end{bmatrix}.$$

c_{12_i} stands for $\cos(q_{1_i} + q_{2_i})$. l_{k_i} and m_{k_i} are the respective lengths and masses of each link.

The following parametrization is proposed for both manipulators

$$\mathbf{Y}(\mathbf{q}, \dot{\mathbf{q}}, \ddot{\mathbf{q}}) = \begin{bmatrix} \ddot{q}_1 & Y_{12} & \ddot{q}_2 & g\mathrm{c}_{12} & g\mathrm{c}_1 \\ 0 & \mathrm{c}_2\ddot{q}_1 + \mathrm{s}_2\dot{q}_1^2 & \ddot{q}_1 + \ddot{q}_2 & g\mathrm{c}_{12} & 0 \end{bmatrix},$$

$$\boldsymbol{\theta} = \begin{bmatrix} \alpha & \beta & \delta & \frac{1}{l_2}\delta & \frac{1}{l_1}(\alpha - \delta) \end{bmatrix}^\top,$$

where $Y_{12} = 2\mathrm{c}_2\ddot{q}_1 + \mathrm{c}_2\ddot{q}_2 - \mathrm{s}_2\dot{q}_2^2 - 2\mathrm{s}_2\dot{q}_1\dot{q}_2$.

The physical parameters for the manipulators are: the length of links $l_{1_i} = l_{2_i} = 0.38$m; the masses for the links are $m_{1_l} = 3.9473$Kg, $m_{2_l} = 0.6232$Kg, $m_{1_r} = 3.2409$Kg and $m_{2_r} = 0.3185$Kg. The initial conditions are $\ddot{\mathbf{q}}_i(0) = \dot{\mathbf{q}}_i(0) = \mathbf{0}$ and $\mathbf{q}_l^\top(0) = [-1/8\pi; 1/8\pi]$, $\mathbf{q}_r^\top(0) = [1/6\pi; -1/4\pi]$ for both controllers. The human operator is modeled as a spring-damper system with gains $K_s = 25$ and $K_d = 5$, respectively. The predefined desired trajectory for the human operator can be seen in Fig.4.

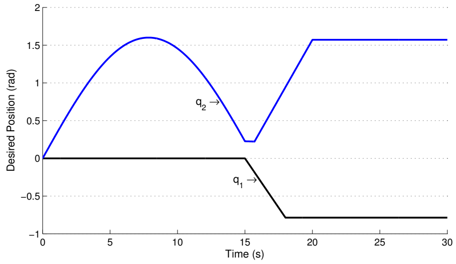

Fig. 4. Desired trajectory of the human operator.

A. Controller Using Acceleration Measurements

For simplicity, as an illustrative example, let us take $\boldsymbol{\lambda} = \mathbf{I}$ in (4), such that the pair $\mathbf{Y}_l, \hat{\boldsymbol{\theta}}_l$, for the local controller (5), becomes

$$\underbrace{\begin{bmatrix} \ddot q_{r,d_1}-\dot e_{l_1} & 0 \\ Y_{21} & Y_{22} \\ \ddot q_{r,d_2}-\dot e_{l_2} & \ddot q_{r,d_1}-\dot e_{l_1}+\ddot q_{r,d_2}-\dot e_{l_2} \\ g\mathrm{c}_{l_{12}} & g\mathrm{c}_{l_{12}} \\ g\mathrm{c}_{l_1} & 0 \end{bmatrix}}_{\mathbf{Y}_l^\top(\mathbf{q}_l,\dot{\mathbf{q}}_l,\mathbf{e}_l,\dot{\mathbf{e}}_l,\ddot{\mathbf{q}}_{r,d},\dot{\mathbf{q}}_{r,d})}, \underbrace{\begin{bmatrix}\hat\alpha_l\\ \hat\beta_l \\ \hat\delta_l \\ \frac{1}{\hat l_{l_2}}\hat\delta_l \\ \frac{1}{\hat l_{l_1}}(\hat\alpha_l-\hat\delta_l)\end{bmatrix}}_{\hat{\boldsymbol\theta}_l}$$

where $Y_{21} = 2\mathrm{c}_{l_2}(\ddot q_{r,d_1} - \dot e_{l_1}) + \mathrm{c}_{l_2}(\ddot q_{r,d_2} - \dot e_{l_2}) - \mathrm{s}_{l_2}\dot q_{l_2}(\dot q_{r,d_2} - e_{l_2}) - 2\mathrm{s}_{l_2}\dot q_{l_2}(\dot q_{r,d_1} - e_{l_1})$ and $Y_{22} = \mathrm{c}_{l_2}(\ddot q_{r,d_1} - \dot e_{l_1}) + \mathrm{s}_{l_2}\dot q_{l_1}(\dot q_{r,d_1} - e_{l_1})$. For the remote controller, the pair $\mathbf{Y}_r, \hat{\boldsymbol{\theta}}_r$ is similar to $\mathbf{Y}_l, \hat{\boldsymbol{\theta}}_l$ with the replacement of the subscript l for r and r, d for l, d.

The controllers gains are $\mathbf{K}_l = 5\mathbf{I}, K_r = 5\mathbf{I}$ and $\boldsymbol{\Gamma}_l = 0.25\mathbf{I}$ and $\boldsymbol{\Gamma}_r = \mathbf{I}$. The time-delays in both paths are set to 0.4s.

The simulations show that position tracking is achieved, moreover, the convergence rate is higher than with only velocity measurements —this effect can be seen when comparing Fig. 5 with Fig. 7. In Fig. 6 the parameter estimation values are presented, the estimation remains bounded and the oscillating behavior is mainly due to changes in the accelerations.

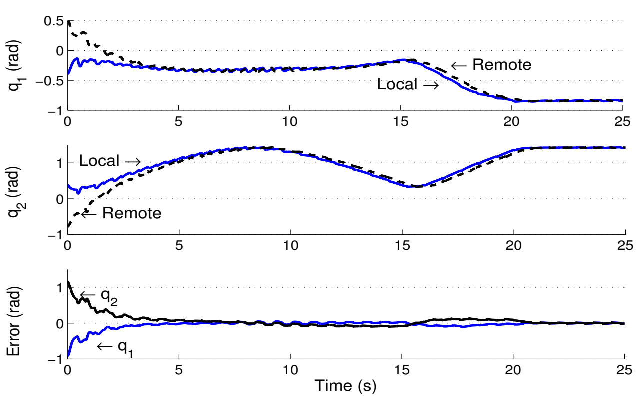

Fig. 5. Joint positions and error of the system controlled using acceleration measurements

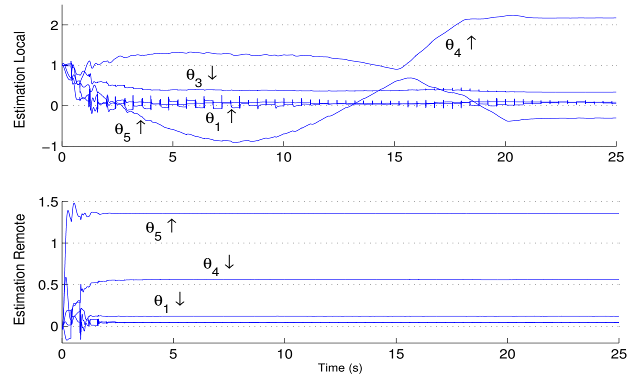

Fig. 6. Parameter estimation of the local and remote manipulators with the scheme that uses acceleration measurements

B. Controller Without Acceleration Measurements

In this case, with $\boldsymbol{\lambda} = \mathbf{I}$ for (8), the matrices $\mathbf{Y}_i$ in (9) are given by

$$\begin{bmatrix} -\dot e_{l_i} & Y_{12} & -\dot e_{i_2} & g\mathrm{c}_{i_{12}} & g\mathrm{c}_{i_1} \\ 0 & -\mathrm{c}_{i_2}\dot e_{i_1} - \mathrm{s}_{i_2}\dot q_{i_1} e_{i_1} & -\dot e_{i_1} - \dot e_{i_2} & g\mathrm{c}_{i_{12}} & 0 \end{bmatrix}$$

where $Y_{12} = -2\mathrm{c}_{i_2}\dot e_{i_1} - \mathrm{c}_{i_2} - \dot e_{i_2} + \mathrm{s}_{i_2}\dot q_{i_2} e_{i_2} + 2\mathrm{s}_{i_2}\dot q_{i_2} e_{i_1}$. The estimation parameters $\hat{\boldsymbol{\theta}}_i$ are the same as in the previous section.

The controllers gains $\mathbf{K}_i$ and $\boldsymbol{\Gamma}_i$, and the time-delays are the same as in the previous section. The extra gain $\mathbf{B} = \mathbf{I}$.

Fig. 7 and Fig. 8 show the evolution of the joint trajectories and the parameter estimations using only velocity and position measurements. Position tracking is achieved and the estimations remain bounded, moreover, the system response is smoother than with the previous controller. Taking a step further, analyzing the velocities of the local and remote manipulators one can conclude that, when employing the controller with acceleration measurements, velocities contain more noise (see Fig. 9 and Fig. 10).

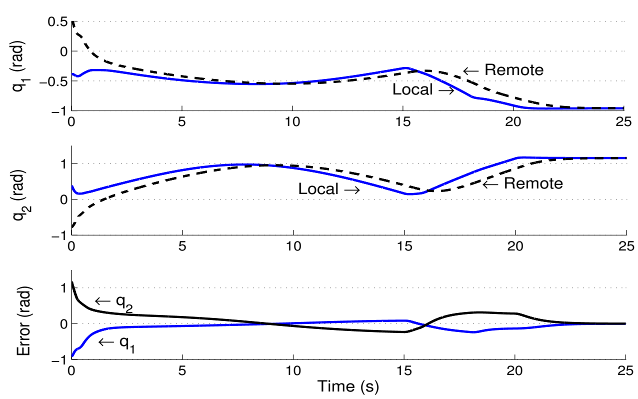

Fig. 7. Joint positions and error of the teleoperator controlled without using acceleration measurements

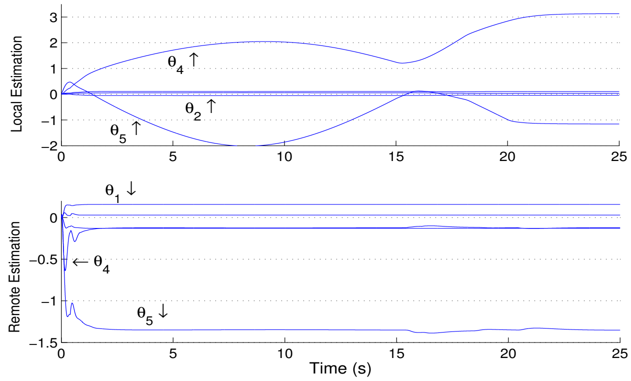

Fig. 8. Parameter estimation of the local and remote manipulators without using acceleration measurements

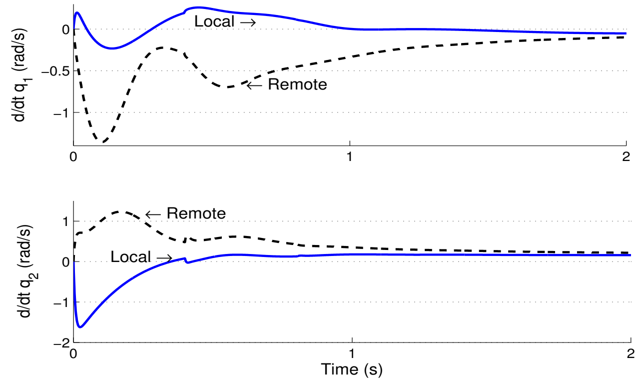

Fig. 10. Joint velocities of the teleoperator controlled without using acceleration measurements

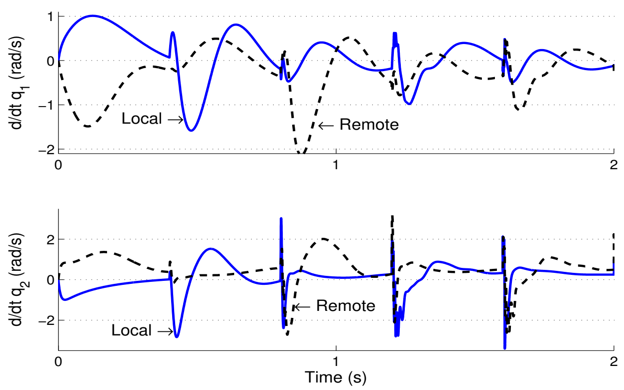

Fig. 9. Joint velocities using the controller with acceleration measurements

V. Conclusions

Two different controllers have been presented in this paper, one using acceleration measurements and the other only velocity and position errors. It has been proved that both can achieve asymptotic convergence to zero of position errors, and are ISS with respect to the input forces of the human operator and the environment. The stability results are independent of constant time-delays. The simulations suggest that, when using accelerations, the tracking performance is better. However, acceleration measurements induce noise resulting on oscillations. A smoother behavior is obtained without the need of accelerations. Future research along adaptive control for teleoperators include the study of the behavior with variable time-delays.

Appendix

Lemma 1: Let $\mathbf{e}, \mathbf{r} \in \mathbb{R}^n$ and $\mathbf{e} = \mathbf{H}(s)\mathbf{r}$, where $\mathbf{H}(s)$ is an $n \times n$ strictly proper, exponentially stable transfer function. Then $\mathbf{r} \in \mathcal{L}_2$ implies that $\mathbf{e} \in \mathcal{L}_2 \cap \mathcal{L}_\infty$, $\dot{\mathbf{e}} \in \mathcal{L}_2$, $\mathbf{e}$ is continuous, and $|\mathbf{e}| \to 0$ as $t \to \infty$. If, in addition, $|\mathbf{r}| \to 0$ as $t \to \infty$, $|\dot{\mathbf{e}}| \to 0$ [11].

Acknowledgements

The authors thank the anonymous reviewers for their valuable comments that, definitely, helped to improve the quality of this paper. This paper has been partially supported by the Spanish CICYT projects DPI2008-02448 and DPI2007-63665, FPI Ref. BES-2006-13393. The first author acknowledges the support of the CONACyT Mexico under the postdoctoral grant 121978.

References

[1] R.J. Anderson and M.W. Spong. Bilateral control of teleoperators with time delay. *IEEE Trans. on Automatic Control*, 34(5):494–501, May 1989.

[2] G. Niemeyer and J.J. Slotine. Stable adaptive teleoperation. *IEEE Journal of Oceanic Engineering*, 16(1):152–162, Jan 1991.

[3] E. Nuño and L. Basañez. Nonlinear bilateral teleoperation: Stability analysis. In *Proc. of the IEEE Int. Conf. on Robotics and Automation*, pages 3718–3723, Kobe, Japan, May 2009.

[4] E. Nuño, R. Ortega, N. Barabanov, and L. Basañez. A globally stable PD controller for bilateral teleoperators. *IEEE Trans. on Robotics*, 24(3):753–758, June 2008.

[5] E. Nuño, L. Basañez, R. Ortega, and M.W. Spong. Position tracking for nonlinear teleoperators with variable time-delay. *The International Journal of Robotics Research*, 28(7):895–910, July 2009.

[6] N. Chopra and M.W. Spong. Output synchronization of nonlinear systems with time delay in communication. In *Proc. of the IEEE Conf. on Decision and Control*, pages 4986–4992, December 2006.

[7] N. Chopra, M.W. Spong, and R. Lozano. Synchronization of bilateral teleoperators with time delay. *Automatica*, 44(8):2142–2148, August 2008.

[8] S.J. Chung and J.J. Slotine. Cooperative robot control and concurrent synchronization of lagrangian systems. *IEEE Trans. on Robotics*, 25(3):686–700, June 2009.

[9] R. Kelly, V. Santibáñez, and A. Loria. *Control of robot manipulators in joint space*. Advanced textbooks in control and signal processing. Springer-Verlag, 2005.

[10] M.W. Spong, S. Hutchinson, and M. Vidyasagar. *Robot Modeling and Control*. Wiley, 2005.

[11] R. Ortega and M. W. Spong. Adaptive motion control of rigid robots: a tutorial. *Automatica*, 25(6):877–888, 1989.

[12] R. Kelly and R. Ortega. Adaptive control of robot manipulators: an input-output approach. In *Proc. of the IEEE Int. Conf. on Robotics and Automation*, volume 2, pages 699–703, April 1988.

[13] M. Vidyasagar. *Nonlinear Systems Analysis*. Prentice Hall, 1993.

[14] I.G. Polushin and H.J. Marquez. Stabilization of bilaterally controlled teleoperators with communication delay: an iss approach. *International Journal of Control*, 76(8):858–870, May 2003.

[15] E. Nuño, R. Ortega, and L. Basañez. An adaptive controller for nonlinear bilateral teleoperators. *Automatica*, 46(1):155–159, January 2010.